Journal of the European Ceramic Society **14** (1994) 131–141

Influence of Formation pH and Grinding of Precursors on Compaction and Sintering Behaviours of 3 mol% Y_2O_3–ZrO_2

A. Samdi,[a,b] B. Durand,[a] A. Daoudi,[b] F. Chassagneux,[a] J. P. Deloume[a]

[a] Laboratoire de Chimie Minérale 3, URA CNRS No. 116, ISTIL, Université Claude Bernard, Lyon I, 43 Boulevard du 11 Novembre 1918, 69622 Villeurbanne Cedex, France
[b] Faculté des Sciences Aîn Chok, Université Hassan II, km 8, Route d'El Jadida, B.P. 5366, Maârif, Casablanca, Morocco

&

M. Taha, J. Paletto, G. Fantozzi

GEMPPM INSA de Lyon, URA CNRS No. 341, 69621 Villeurbanne Cedex, France

(Received 27 September 1993; accepted 2 February 1994)

Abstract

Tetragonal stabilized zirconia samples, 3 mol % in Y_2O_3, are prepared by pyrolysis up to 900°C of gelatinous precursors formed by hydrolysis of aqueous solutions containing both zirconium and yttrium acetates. Such prepared powders are white, but still contain about 0·5 wt % in carbon.

The increase of the end hydrolysis pH from 3·9 to 10·0 has a very limited influence on the evolution of the density of samples during cold compaction and then sintering by heating at 1500°C.

The ball-milling of the precursor before pyrolysis decreases the size of the agglomerates formed at 900°C without modifying the size of crystallites. The size of large interagglomerate pores is also decreased. The whole porosity remains constant and only the distribution between open and closed porosity is modified. The modification of the morphology eases the gaseous release during heating and leads to a more significant shrinkage and consequently to a higher density after sintering.

Zirkoniumoxidproben, 3 mol % Y_2O_3–ZrO_2, in tetragonaler Form stabilisiert, werden durch Pyrolyse bei 900°C gelartiger Ausgangsprodukte die durch Hydrolyse wässeriger Yttrium und Zirkoniumacetatlösungen erzeugt sind, hergestellt. Die so erhaltenen Pulver sind weiss, enthalten aber noch etwa 0·5 % (in Gew.) Kohlenstoff.

Die pH-Erhöhung am Ende der Hydrolyse von 3·9 auf 10·0, hat nur einen beschränkten Einfluß auf die Fortentwicklung der Dichte der Proben beim Verdichten in der Kälte und danach beim Sintern bei 1500°C.

Das Vermahlen des Ausgangsprodukts vor der Pyrolyse verringert die Grösse der bei 900°C gebildeten Agglomerate ohne die Grösse der Kristallite zu verändern. Der Umfang der grossen Poren zwischen der Agglomeraten ist auch vermindert. Die Gesamtporosität bleibt unverändert und allein die Aufteilung zwischen offerner und geschlossener Porosität ist verändert. Die Morphologieveränderung erleichtert die Entwicklung der während des Erhitzens entstandenen Gase und führt zu einem bedeutenderen Schwinden und somit zu einer höheren Dichte nach dem Sintern.

Des échantillons de zircone stabilisée sous forme quadratique, 3 mol % Y_2O_3–ZrO_2, sont préparés par pyrolyse à 900°C de précurseurs gélatineux formés par hydrolyse de solutions aqueuses d'acétates d'yttrium et de zirconium. Les poudres ainsi obtenues sont blanches, mais renferment encore environ 0·5% en poids de carbone.

L'élévation du pH de fin d'hydrolyse de 3·9 à 10·0 n'a qu'une influence très limitée sur l'évolution de la densité des échantillons lors de la compaction à froid, puis du frittage par chauffage à 1500°C.

Le broyage du précurseur avant pyrolyse diminue la taille des agglomérats formés à 900°C sans modifier la taille des cristallites. La taille des gros

Journal of the European Ceramic Society 0955-2219/94/$7.00

pores inter-agglomérats est également diminuée. La porosité totale reste constante et seule la répartition entre porosité ouverte et porosité fermée est modifiée. La modification de la morphologie facilite le départ des gaz formés pendant le chauffage et conduit à un retrait plus important, donc à une meilleure densité après frittage.

1 Introduction

A simple route for preparation of yttrium stabilized zirconia is the hydrolysis of zirconyl and yttrium acetates solutions leading by evaporation to amorphous precursors and then by pyrolysis to tetragonal 3 mol % Y_2O_3–ZrO_2 solid solutions.[1]

Recently, for zirconia samples prepared by pyrolysis of precursors corresponding to a hydrolysis ratio r = 0·9 (r = moles OH^- added/initial moles Zr + Y), the best results[2] in sintering were obtained without diluting the starting commercial zirconyl acetate solution and using ammonia concentration ranging from 1·3 to 2·8 mol/litre.

The present paper is concerned with the study of the influence, on zirconia sintering behaviour, of the pH of formation of the wet precursor and the grinding of the dry precursor before pyrolysis.

In the previous investigation,[2] pH, corresponding to a hydrolysis ratio r = 0·9, depended upon ammonia concentration and varied from 6·3 to 6·9.

2 Experimental

Five dry precursors were prepared starting from the commercial zirconyl acetate solution (Riedel de Haen, 22 wt% in ZrO_2, pH = 3·3) in which solid yttrium acetate was dissolved so as to get a molar ratio $Y_2O_3/(Y_2O_3 + ZrO_2)$ = 0·03; the pH increased to 3·9. The hydrolysis was performed by adding a 2·2 mol/litre ammonia solution until various hydrolysis ratios in the range 0–4·1 were reached (Table 1). Acidic samples A and B were in the form of a viscous solution; neutral sample C was a gelatinous solid; basic samples D and E were in the form of milky solutions. All dry precursors were obtained by evaporating on a sand bath at 80–90°C for 15 h.

The elemental analysis of the dry precursors

Table 1. Synthesis parameters of various precursors

Sample	*pH*	*r*
A	3·9	0
B	5·8	0·6
C	6·7	0·9
D	9·2	1·6
E	10·0	4·1

Table 2. Elemental analysis of dried precursors

Sample	*Analysis*				
	Weight (%)				*Molar ratio*
	Zr	*C*	*H*	*N*	CH_3COO/Zr
A	41·9	15·2	3·2	<0·3	1·4
B	39·3	14·2	3·1	0·6	1·4
C	40·5	15·4	3·5	1·0	1·5
D	39·8	13·3	2·8	0·4	1·3
E	41·3	11·4	3·2	<0·3	1·1

(Table 2) indicated that the amount of nitrogen was maximum for the gelatinous sample C and that the pH rise, from 3·9 to 10·0, decreased the ratio CH_3COO/Zr.

The dry precursors were either used as obtained (A1–E1) or submitted to a ball-milling for 30 min with alumina balls (A2–E2). Then pyrolysis was followed by TGA and DTA coupled to a mass spectrometer. The resulting zirconia powders were characterized (XRD, sedimentation speed measurements, mercury porosimetry, BET and SEM) and their compaction and sintering behaviours were investigated (compaction test, dilatometry) using the same apparatus as in the previous study[2]. In no case, were zirconia samples ground.

3 Results

3.1 Pyrolysis of dried precursors and characteristics of zirconia powders

As for the previously studied precursors,[2] the transformation of dried precursors into white zirconia powders requires calcination up to 900°C. X-ray patterns then give clear evidence for the formation of a single phase of yttrium tetragonal stabilized zirconia. Thermogravimetric analysis (Fig. 1), coupled with identification of the gaseous release by mass spectrometry, indicates that the pyrolysis involves three steps:

—Firstly, the dehydration occurring between 50 and 250°C and giving a weight loss of 10–20%.

—Secondly, the decomposition of the acetate radical giving a second weight loss of about 20% and corresponding to a release of H_2O, CO_2 and CH_3–CO–CH_3; it begins at 250°C and is ended at about 550°C for the ball-milled samples (Fig. 1(b)) and 650°C for the other samples (Fig. 1(a)); for the latter, the more acid the sample the slower the decomposition rate; in any case, the grey colour of the residue indicates that carbon has not been completely eliminated.

—Finally, a third small weight loss (2–3%) due

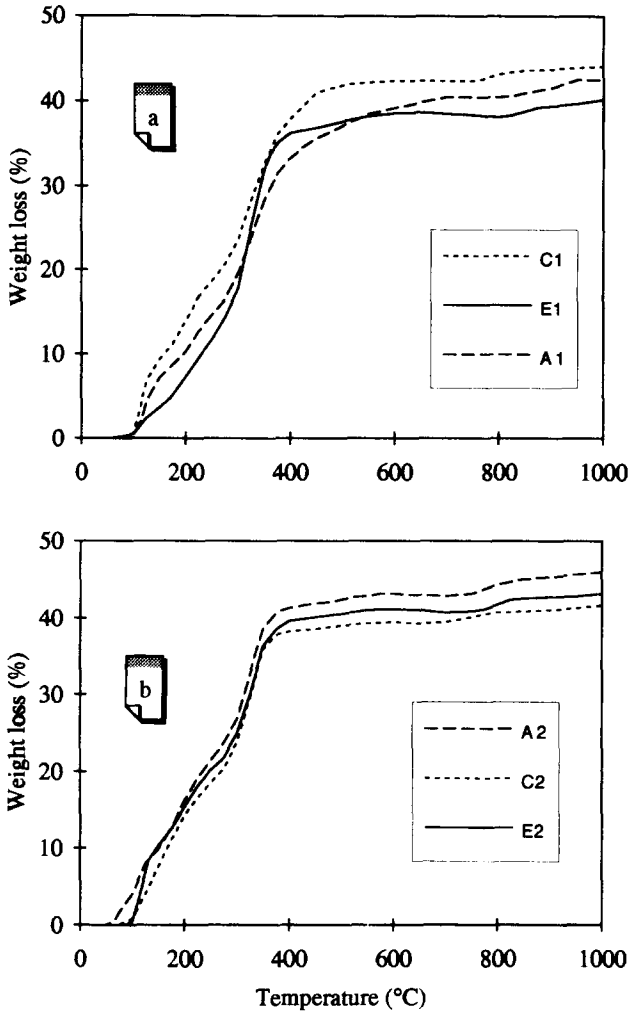

Fig. 1. TGA curves (150°C/h) of dried precursors A, C and E; (a) non-ground samples A1, C1, E1; (b) ball-milled samples A2, C2, E2.

to a release of CO_2 and H_2O and revealing a further elimination of carbon leading to white zirconia powders; this loss occurs in the range 800–900°C for non ground samples A1–E1, 700–800°C for ball-milled samples A2–E2.

The comparison between Fig. 1(a) and (b) shows that the mechanical grinding slightly increases the amount of water lost during the first step and shifts the end of the decomposition of the acetate radical, particularly the second elimination of carbon, towards low temperatures. The influence of ball-milling is also shown on the DTA curves (Fig. 2, Table 3). For both types of samples, the dehydration is revealed by several endothermic peaks in the range 50–350°C which are not modified by the milling. On the contrary, the decomposition of acetate radical produces several exothermic effects for samples A1–E1 in the range 350-650°C and only one significant exothermic effect between 350 and 400°C for samples A1–E2. The last elimination of carbon is indicated by a weakly exothermic effect close to 950°C for samples A1–E1 and to 850°C for samples A1–E2, confirming the decrease of temperature due to grinding. Moreover, it is noticed that the higher the pH of formation of the gel is, the lower the temperature of carbon elimination is.

Table 3. Temperatures of DTA peaks

Samples	*Peak temperature (°C)*	
	Endothermic effects	*Exothermic effects*
A1	105, 230, 305, 340	380, 410, 510, 605, 970
C1	85, 180, 320	360, 415, 485, 540, 935
E1	105, 215, 335	385, 490, 555, 820
A2	85, 195, 280	365, 495, 555, 865
C2	85, 180, 300	370, 490, 555, 870
E2	85, 195, 300	385, 495, 560, 840

Heating rate in air 600°C/h.

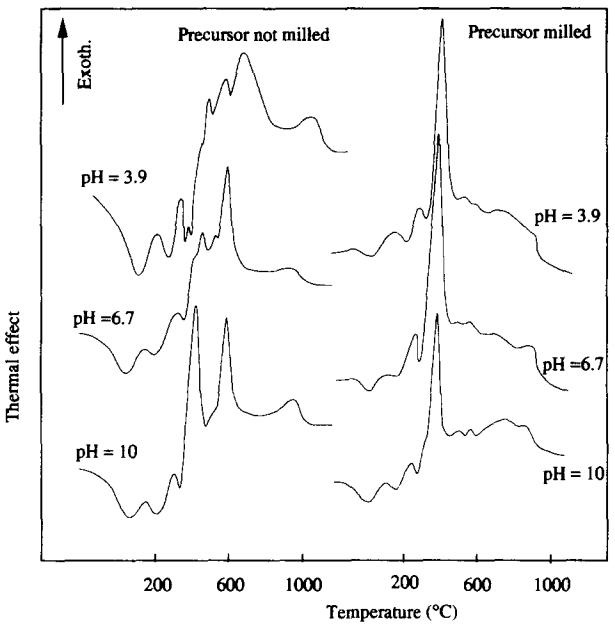

Fig. 2. DTA curves (600°C/h) of dried precursors A, C and E; (left) non-ground samples A1, C1, E1; (right) ball-milled samples A2, C2, E2.

Some characteristics of zirconia powders obtained by pyrolysis in air up to 900°C at a rate of 150°C/h are gathered in Table 4. Although the pyrolysis leads to white zirconia powders, they still contain carbon amounts of about 0·5 wt %. Owing to the temperature of calcination, powders exhibit low specific surface areas which seem independent of the pH of formation of the precursor and are not affected by the mechanical grinding. The same observations are valid for crystallite size. The difference between surface areas measured by nitrogen adsorption (BET) and mercury penetration must be attributed to the existence of pores with radii lower than 3·8 nm, too narrow for mercury penetration at 200 MPa. The increase, due to the ball-milling, of the surface area determined from mercury penetration is consistent with the decrease of the mean size of the agglomerates. Considering the small size of crystallites and the

Table 4. Characteristics of zirconia powders obtained by pyrolysis, up to 900°C, of the precursors

Sample	*Characteristics*					
	Precursor formation pH	*C (weight %)*	*Specific surface area (m^2/g)*		*Agglomerates mean diameter (μm)*	*Crystallites, mean diameter (nm)*
			BET	*Mercury porosimetry*		
A1	3·9	0·4	4	1·5	4·8	21·5
B1	5·8	0·5	5	1·2	4·6	22·0
C1	6·7	0·5	6	2·6	3·5	20·0
D1	9·2	0·5	6	2·0	3·7	22·0
E1	10·0	0·3	5	0·5	3·6	25·0
A2	3·9	0·5	7	3·7	1·7	25·5
B2	5·8	0·5	7	4·8	1·6	25·0
C2	6·7	0·4	6	2·3	1·5	25·5
D2	9·2	0·4	5	3·2	1·4	25·5
E2	10·0	0·4	6	2·0	1·5	26·0

low BET surface area, it is unambiguously to be concluded that the elementary grains are polycrystalline; if the grains were monocrystalline a diameter of 20 nm would give a surface area of 50 m^2/g. As previously reported,[3,4] the small size of crystallites could be assigned to the presence of residual carbon limiting their growth.

The determination of granulometric distributions, by sedimentation speed measurements, separates zirconia samples into three groups (Fig. 3):

—First group, samples A1 and B1: coarse powders with sizes in the range 0·5–18·0 μm and mean diameters close to 4·7 μm.
—Second group, samples C1, D1 and E1: intermediate powders with sizes lower than 15 μm and mean diameters close to 3·6 μm.
—Third group, samples A2, B2, C2, D2 and E2: fine powders with sizes lower than 5 μm and mean diameters close to 1·5 μm.

3.2 Compaction behaviour

As previously noticed,[2] compaction curves of zirconia powders, d versus ln (P), where d is the relative density expressed in % of the theoretical density and P the applied uniaxial pressure (Fig. 4), are characterized by two linear domains separated by a breaking pressure P_j. The first linear variation at low applied pressures is due to a slide of agglomerates on each other involving an inter-agglomerates rearrangement depending upon their shape, their density and their size distribution.[5] The second one is governed by the deformation and/or the breaking of agglomerates beginning at

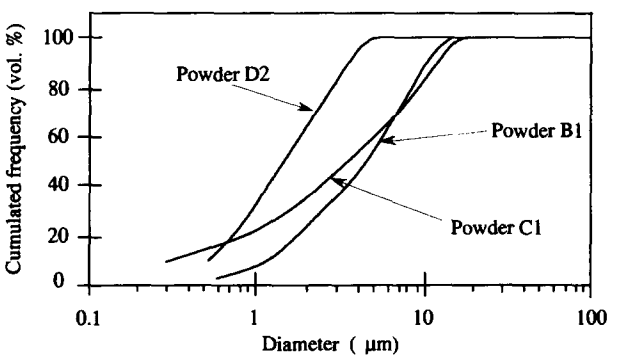

Fig. 3. Granulometric curves of zirconia samples D2, B1 and C1 obtained by pyrolysis, up to 900°C, of precursors.

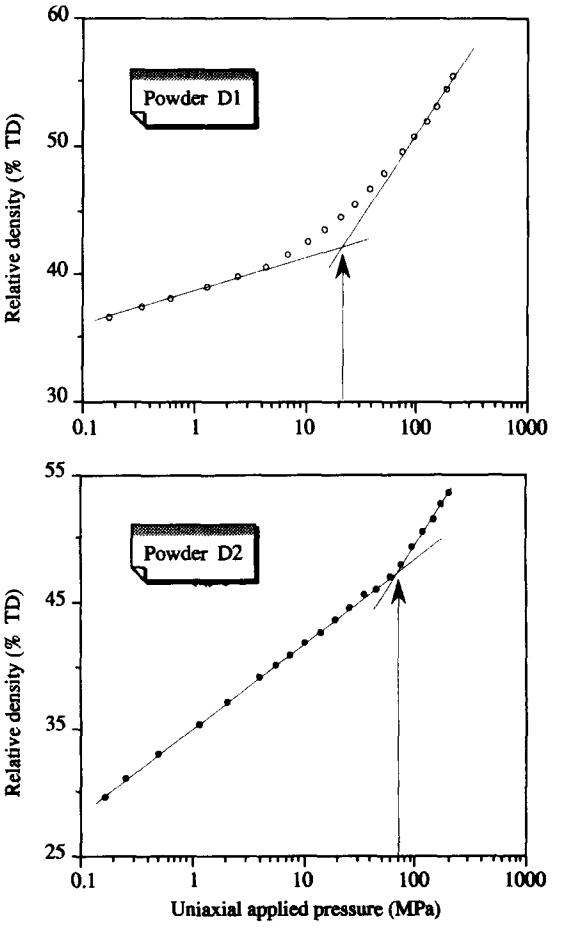

Fig. 4. Compaction curve of zirconia samples D1 and D2.

Table 5. Compaction data

Sample	*Data*				
	Slope of low pressure linear area (% TD/MPa)	*Slope of high pressure linear area (% TD/MPa)*	*Threshold pressure P_j (MPa)*	*Density (% TD)*	
				Starting powder	*Compacted pellet (at 215 MPa)*
A1	2·9	17·0	24	35·2	56·9
B1	2·6	12·0	30	37·7	55·1
C1	1·9	12·7	16	37·1	56·2
D1	2·8	13·1	21	37·2	54·8
E1	2·9	13·0	20	38·1	56·1
A2	7·0	13·9	80	28·1	53·6
B2	6·2	13·9	60	26·3	54·4
C2	6·2	13·6	70	28·2	54·1
D2	6·7	12·3	7	26·9	54·0
E2	6·5	14·1	75	26·8	54·1

the threshold pressure P_j and inducing the partial elimination of the interagglomerates porosity.[6] The value of the pressure P_j is highly sensitive to the hardness of agglomerates.

Compaction data are summarized in Table 5. The five powders A1–E1 exhibit similar compaction behaviours characterized by threshold pressures P_j close to 25 MPa and by powder densities increasing from 37 to 56% of the theoretical density as the applied pressure is raised up to 215 MPa. The five powders A2–E2 also present similar compaction behaviours distinguished by threshold pressures P_j higher than 70 MPa and by powder densities increasing from 27 to 54% of the theoretical density. Therefore as shown in Fig. 4, the decrease of agglomerates size produced by the ball-milling involves simultaneously a lowering of initial powder density and an important shift of the threshold pressure P_j towards high pressures. Densities obtained after uniaxial pressing up to 215 MPa are slightly lower for ball-milled powders and, in other respects, a cleavage of the corresponding pellets is noticed.

3.3 Sinterability

Powders were uniaxially pressed up to 100 MPa and then isostatically up to 400 MPa, so as to avoid cleavage of pellets inherent to uniaxial pressing at high pressure. Dilatometric curves were recorded heating up to 1500°C at a rate of 60°C/h, maintaining the temperature for 3 h and finally cooling at the same rate.

The observation of the dilatometric data (Table 6) reveals similarities in the behaviour of the powders A1–E1, on the one hand, and the powders A2–E2 on the other hand. For the latter, the thermal treatment increases the density from a green value close to 3·38 to a sintered value reaching about 5·33 and involves a linear shrinkage close to 15% and a firing loss of about 4·3%. For the former, the density is increased from 3·48 to 4·8 and the shrinkage and the firing loss are respectively 12·3% and 2·8%.

As shown in Fig. 5(a) for samples D1 and D2, taken as example of the two series of powders, a small expansion occurs for both powders, in the range 20–900°C, probably due to the elimination of superficial adsorbed water and to the dilatation of the material. For powders A2–E2, a second expansion is observed between 900 and 1000°C, whereas for powders A1–E1 the shrinkage begins as soon as 900°C is reached. Beyond 1000°C powders A2–E2 exhibit a regular shrinkage when, for powders A1–E1, a significant decrease of the sintering rate is noticed close to 1200°C; it was previously attributed[2,7] to the gaseous release produced by the elimination of residual carbon, present in the state of carbonate or oxycarbonate. For both powders, the sintering is not ended at 1500°C, as revealed by the shrinkage during the isothermal level (Fig. 5(b)). The difference observed between A1–E1 and A2–E2 is the consequence of the ball-

Table 6. Sintering data (1500°C, 3h)

Sample	*Data*			
	Density (% TD)		*Shrinkage (%)*	*Firing loss (%)*
	Green	*Sintered*		
A1	58·0	80·3	11·6	2·8
B1	57·7	78·7	10·9	2·5
C1	57·4	77·0	12·3	2·9
D1	56·2	77·0	12·5	2·9
E1	56·4	78·7	12·4	2·8
A2	55·4	87·2	15·0	4·4
B2	55·4	87·7	15·5	4·5
C2	55·7	87·4	15·5	3·9
D2	55·7	86·9	15·0	4·5
E2	54·4	87·4	15·5	4·2

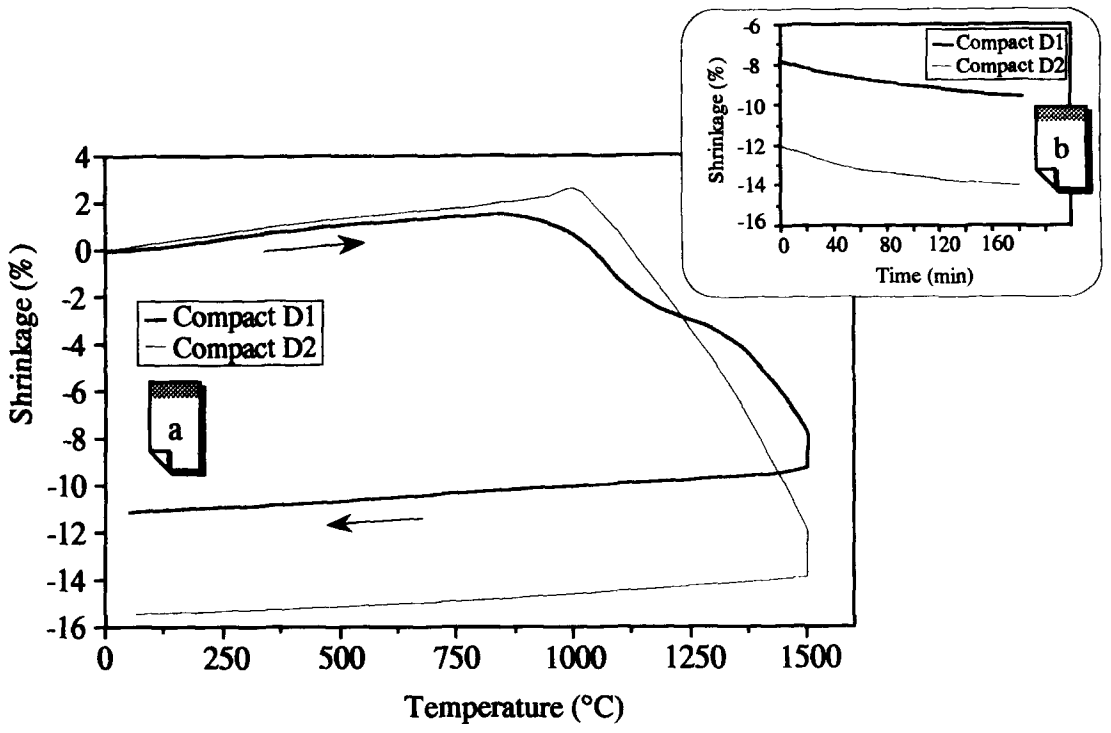

Fig. 5. Dilatometric curves (60°C/h) of samples D1 and D2; (a) heating and cooling stages; (b) isothermal level at 1500°C.

milling of precursors which provides an easier elimination of carbon. In any case destabilization of tetragonal zirconia is never observed on the cooling curves (Fig 5(a)).

3.4 Thermogravimetric analysis of green compacts

Chemical analysis of carbon content (Table 4) gives comparable values for samples A1–E1 and A2–E2. However, TGA, performed at a rate of 150°C/h on green pellets isostatically pressed up to 400 MPa, shows a difference in the behaviour of powders A1–E1 and A2–E2, as illustrated for samples D1 and D2 (Fig. 6). Below 500°C, a small loss of adsorbed water is observed. The next, one due to the elimination of residual carbon revealed by mass spectrometry, arises above 900°C. It appears more intense for powders A2–E2 than for powders A1–E1. In both cases carbon elimination is not ended when the temperature reaches 1500°C.

3.5 Mercury porosimetry investigation of green and sintered compacts

Two kinds of porosity are observed, an inter-agglomerates porosity with pore sizes greater than 30 nm and an intra-agglomerate porosity with pore sizes lower than 10 nm. The open porosity is deduced from mercury penetration; the whole porosity is determined from measurement of the size for green pellets and from pycnometry

Table 7. Green compacts porosity

Sample	*Whole porosity (mm^3/g)*	*Open porosity (mm^3/g)*	*Pore radii (nm)*	*Closed porosity (mm^3/g)*
A1	118·6	89·8	*30–2500 (maximum penetration at 290) *3·8–10	28·8
B1	120·2	93·7	*30–2500 (maximum penetration at 470) *3·8–100	26·5
C1	121·8	97·7	*30–2500 (maximum penetration at 470) *3·8–100	24·1
D1	127·6	99·1	*30–2500 (maximum penetration at 470) *3·8–100	28·5
E1	126·8	77·5	*30-2500 (maximum penetration at 470)	49·3
A2	131·9	98·3	*10–240 (maximum penetration at 90) *3·8–100	33·6
B2	131·9	96·2	*10–240 (maximum penetration at 100) *3·8–10	35·7
C2	130·2	91·8	*3·8–190 (maximum penetration at 120)	38·4
D2	129·2	98·7	*10–240 (maximum penetration at 90)	31·5
E2	137·3	88·0	*3·8–240 (maximum penetration at 110)	49·3

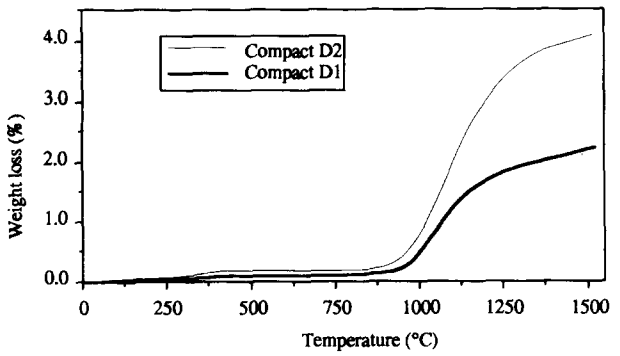

Fig. 6. TGA curves (150°C/h) of zirconia green compacts, samples D1 and D2.

for sintered materials; the closed porosity is obtained by difference. From data gathered in Table 7 for green samples and in Table 8 for sintered samples and reported as mercury penetration versus pore radius curves (Figs 7 and 8). samples A1–E1 can be distinguished from ball-milled powders A2–E2.

3.5.1 Behaviour of samples A1–E1

For green samples A1–E1, the representation of Hg penetration versus pore radius, Fig.7(a), shows the existence of two kinds of pores with radii spread in the ranges 3·8–10·0 nm and 30–2500 nm, respectively. A slight increase of the whole porosity as the basicity is raised from pH = 3·9 to pH = 10·0 (Table 7, Fig. 7(a)) is seen. Intra-agglomerate porosity is not observed for the most basic sample E1, which exhibits the highest closed porosity obtained; the lowest one is observed for the quite neutral sample C1.

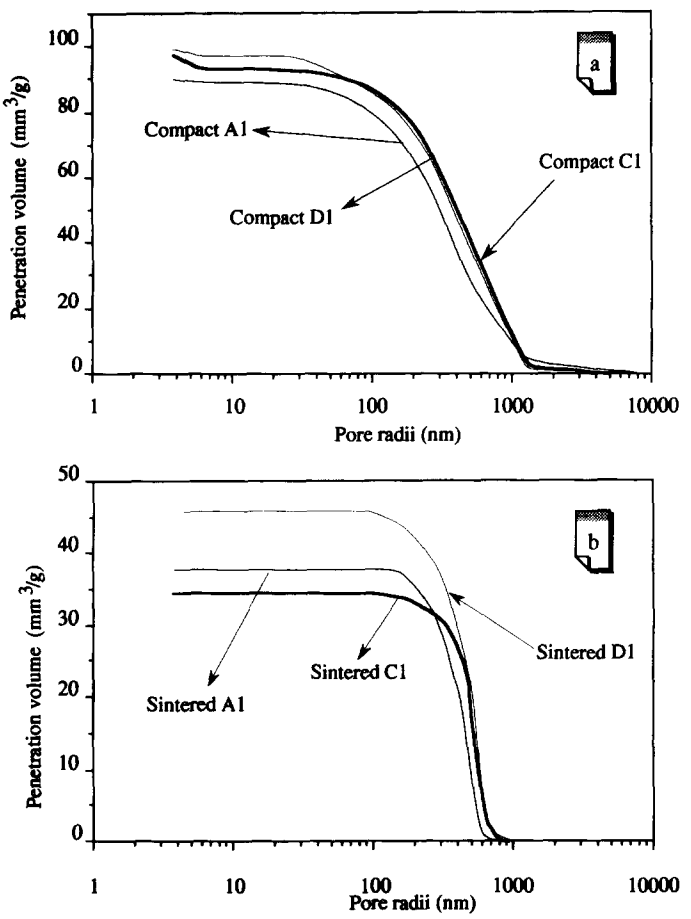

Fig. 7. Mercury penetration curves of (a) green pellets A1, C1, D1; (b) sintered pellets A1, C1, D1.

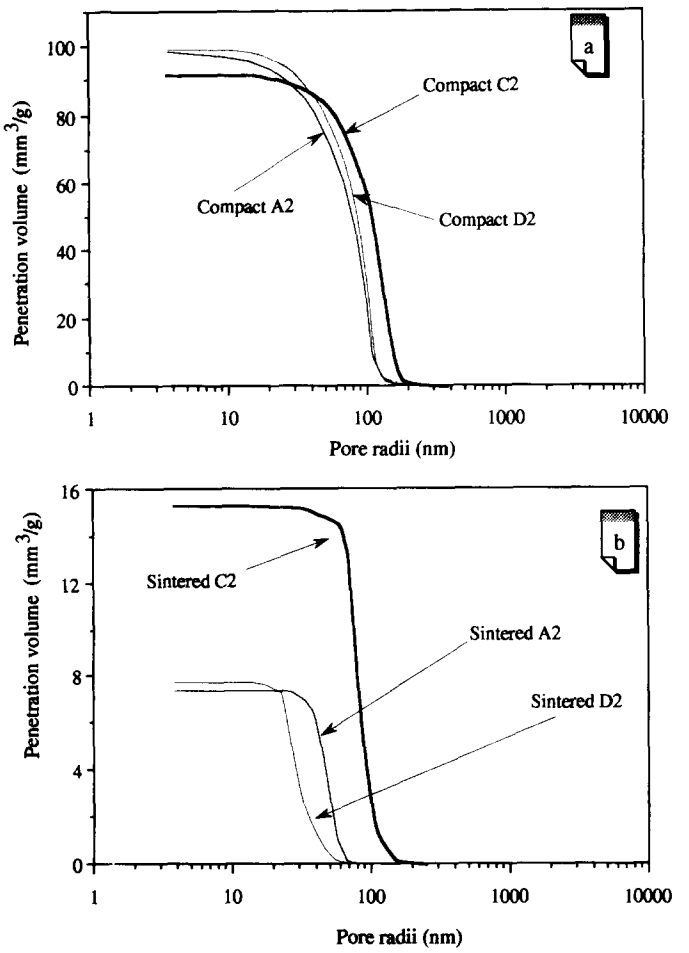

Fig. 8. Mercury penetration curves, (a) green pellets A2, C2, D2; (b) sintered pellets A2, C2, D2.

A lowering of the whole porosity of about two-thirds is involved by sintering at 1500°C for 3 h and (Table 8, Fig. 7(b)), the vanishing of intra-agglomerate porosity, the decrease of about 50% of the open porosity and a drastic decrease of the closed one, are noticed. The closed porous volume becomes lower than 2·5 mm^3/g, except for the densified sample C1, for which it reaches 13·6 mm^3/g, whereas its green pellet gave the lowest value (24·1 mm^3/g). In addition, the spread of pore radii is significantly narrowed with only small changes in the maximum penetration radii.

3.5.2 Behaviour of samples A2–E2

In green compacts prepared from ball-milled precusors A2–E2, the intra-agglomerate porosity is detected only for the two more acidic samples A2 and B2 (Table 7, Fig. 8(a)). Another effect of ball-milling is a strong decrease of pore radii, now situated in the range 10–240 nm with a maximum of penetration between 90 and 120 nm (Fig. 8(a)).

Table 8. Sintered pellets porosity

Sample	*Whole porosity (mm^3/g)*	*Open porosity (mm^3/g)*	*Pore radii (nm)*	*Closed porosity (mm^3/g)*
A1	40·1	37·7	170–750 (maximum penetration at 470)	2·4
B1	48·8	47·3	180–750 (maximum penetration at 540)	1·5
C1	47·9	34·3	250–940 (maximum penetration at 470)	13·6
D1	48·8	45·7	190–750 (maximum penetration at 540)	3·1
E1	44·4	43·4	160–625 (maximum penetration at 420)	1·0
A2	24·0	7·3	25–65 (maximum penetration at 50)	16·7
B2	23·0	10·3	15–125 (maximum penetration at 30)	12·7
C2	23·7	15·3	30–125 (maximum penetration at 70)	8·4
D2	24·7	7·6	15–65 (maximum penetration at 30)	17·1
E2	23·7	0·0	—	23·7

The open porous volume is not affected and remains close to 95 mm^3/g. The closed porous volume is slightly increased, except for sample E2, for which it reaches the same highest value as for sample E1, 49 mm^3/g.

The ball-milling of precursors promotes the decrease of the whole porous volume produced by the sintering at 1500°C for 3 h, so that the values obtained for samples A2–E2 (24 mm^3/g for all samples) appear about twice as low as for samples A1–E1, (Table 8, Fig. 8(b)). An opposite variation of open and closed porosity is noticed (Fig. 9); the more basic sample E2 exhibits only a closed porosity. The decrease profits the open porosity all the more, the closed one appearing generally higher for samples A2–E2 than for sintered samples A1–E1. As for samples A1–E1, a very significant narrowing of pore radii spread and a decrease of the maximum of penetration are observed.

4 Discussion

From the comparison of specific surface areas of zirconia samples determined by nitrogen adsorption (BET) and mercury penetration. it is noticed that the ball-milling of the precursors increases significantly the Hg areas (particularly for samples A, B and E) whereas it has quite no influence on BET areas. Thus, it appears clearly that the area calculated from Hg porosimetry data is due principally to the interagglomerates porosity which is strongly affected by the decrease of the size of the agglomerates and perhaps by a modification of their shape. In contrast, the area calculated from BET data is essentially due to the intra-agglomerates porosity related to the size of elementary grains or crystallites and perhaps to their own microporosity.

The decrease of the size of agglomerates and of the size of the interagglomerates pores influences both compaction and sintering behaviours of zirconia powders. For compaction, the main difference is revealed by the shift of P_j towards high pressures, indicating that agglomerates in powders A2–E2 are more difficult to break or to distort and then smaller and harder than those of powders A1–E1. At pressures lower than P_j, the higher slope for samples A2–E2 is consistent with an easier rearrangement of the small agglomerates inside the matrix. After isostatic pressing at 400 MPa, green compacts A1–E1 and A2–E2 exhibit comparable porous volumes, but the size distribution is significantly narrowed by the milling of the precursors. Consequently, the fine porosity of green pellets A2–E2 (radii lower than 240 nm) allows a regular elimination of gaseous compounds formed above 1000°C during the sintering. The slightly lower green densities of pellets A2–E2 are balanced by a higher shrinkage leading to higher densities. In contrast, for samples A1–E1, the coarser green porosity (size in the range 30–2500 nm) is more difficult to eliminate by volumic

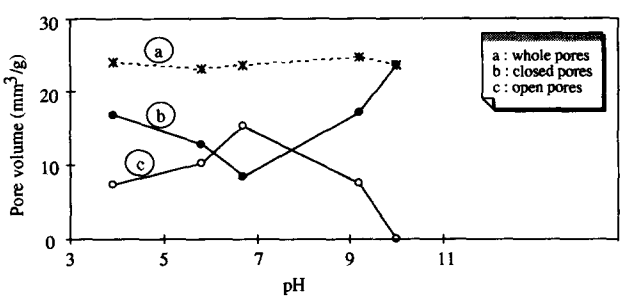

Fig. 9. Variation of pore volume versus pH for samples obtained from the ball-milled precursors.

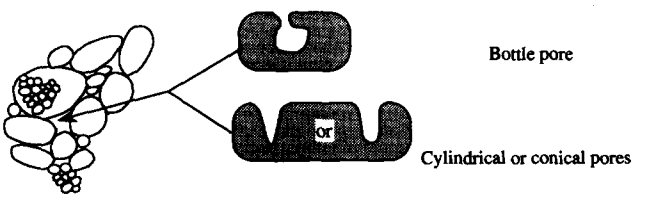

Fig. 10. Porosity type in green compacts D1 and D2.

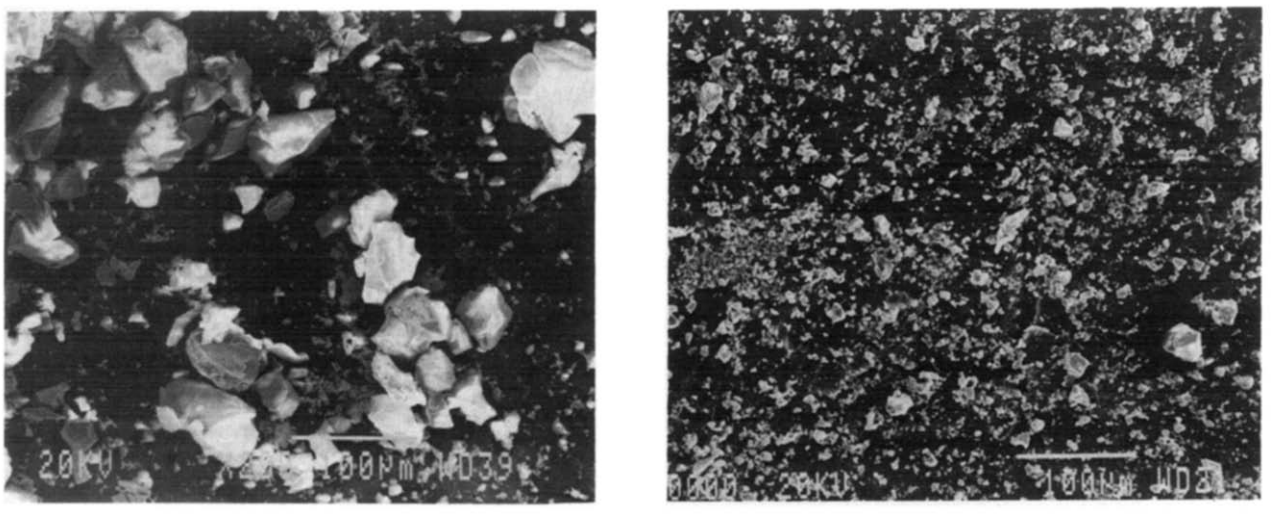

(a) (b)

Fig. 11. SEM micrographs of powders (a) D1 and (b) D2 obtained by pyrolysis of precursors up to 900°C.

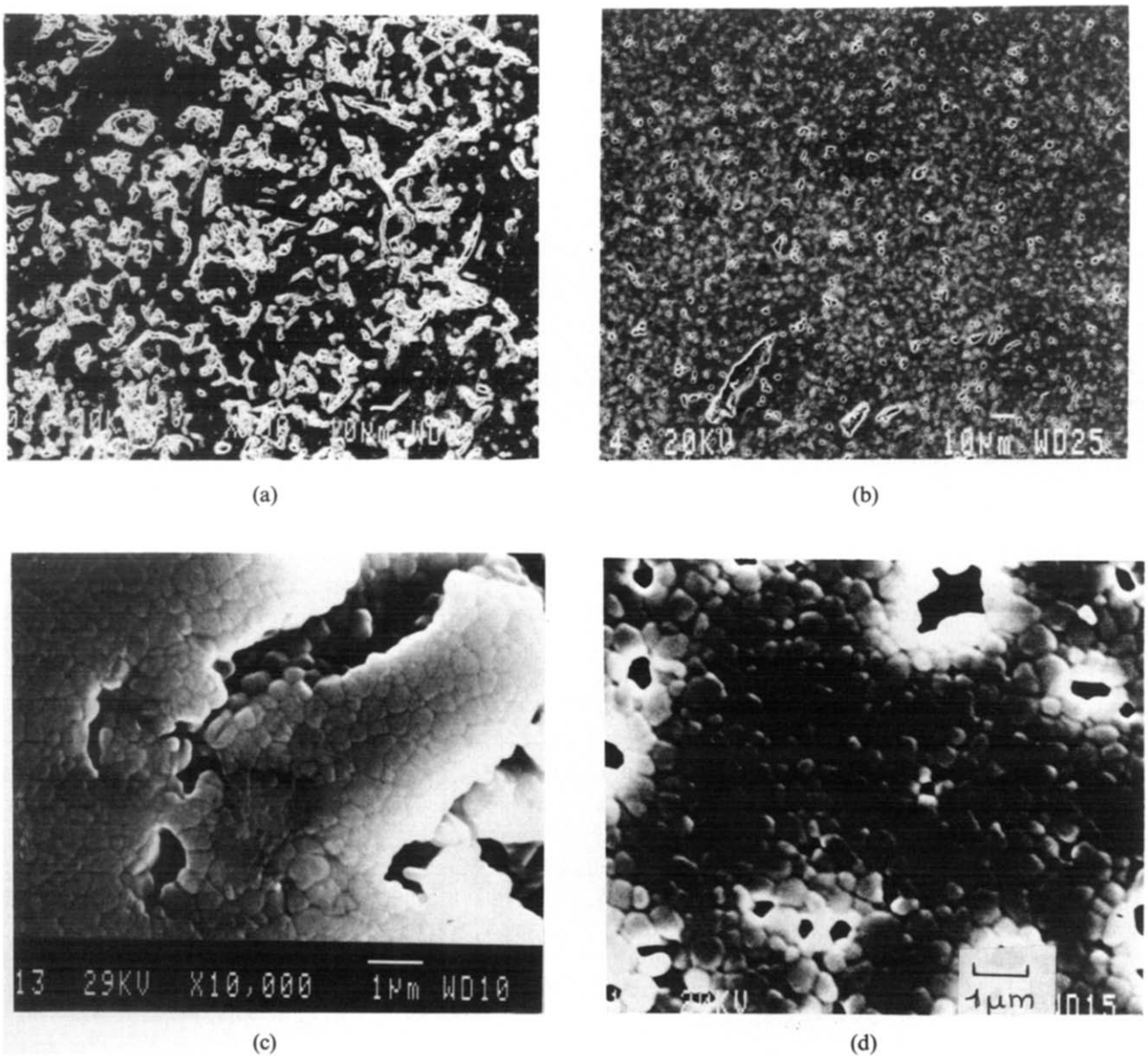

(a) (b)

(c) (d)

Fig. 12. SEM micrographs of polished sections of sintered bodies (1500°C, 3 h) of samples D1 ((a) and (c)) and D2 ((b) and (d)).

diffusion and only poor sintered densities are achieved, although the bodies exhibit a very low closed porosity.

Another influence of ball-milling is noticed looking at the evolution of porosity during sintering. The presence of a higher closed porosity and of a lower open porosity in sintered samples A2–E2 than in sintered samples A1–E1, could be interpreted assuming that in green compacts A2–E2 the interagglomerates pores are bottle-shaped, whereas those of green compacts A1–E1 are cylindrical or cone-shaped (Fig. 10). Owing to their smaller size and to their shape, the bottle-shaped open pores of green pellets A2–E2 would be liable to close, whereas the large cylindrical or conical pores of green pellets A1–E1 would not be affected by sintering.

Electron micrographs corroborate the preceding interpretation. For the powders, they reveal clearly the decrease of the size of the agglomerates involved by the milling of the precursors as shown on Fig. 11 for the powders D1 and D2. For sintered bodies, electron micrographs (Fig. 12) of a polished section show a regular intra-agglomerate sintering for both kinds of powders: a more significant and regularly distributed closed porosity for A2–E2, on the one hand, and a poor inter-agglomerate sintering, particularly in case of A1–E1, on the other hand.

5 Conclusion

The formation of white yttrium stabilized zirconia powders, by pyrolysis of precursors obtained by hydrolysis at different pH, of aqueous solutions containing both zirconium and yttrium acetate, requires thermal treatments up to 900°C so as to eliminate the major part of carbon. These zirconia powders are constituted of large agglomerates with mean diameters close to 4 μm and extended size distribution; they still contain amounts of about 0·5 wt% carbon. Isostatic compaction up to 400 MPa leads to green pellets characterized by a coarse interagglomerates porosity, with extended size distribution and mean radius close to 470 nm, and by an intra-agglomerate porosity in the range 3·8–10·0 nm; agglomerates are broken or distorted above 20 MPa. The firing of green pellets at 1500°C for 3 h involves a homogeneous intra-agglomerate sintering, leading to a very low closed porosity (porous volume <3 mm^3/g), but it has quite no influence on the interagglomerates porosity; the pore size distribution is indeed narrowed but the mean size remains unchanged. During sintering, residual carbon is eliminated by formation of gaseous compounds which produce an inflation because their release is made difficult by the evolution of the porosity. Shrinkage rate is simultaneously decreased and only poor densities are achieved (80% TD).

The ball-milling of precursors decreases the size of the agglomerates formed by pyrolysis up to 900°C. The whole porous volume is not changed but the size of large interagglomerates pores is decreased and distribution in size narrowed while intra-agglomerate porosity is not affected. The modifications of the morphology of zirconia powders strongly influence their compaction and sintering behaviours. The compaction rate is increased and the breaking of agglomerates shifted towards higher pressures. The firing at 1500°C for 3 h involves simultaneously a homogeneous intra-agglomerate sintering, as for non-ground samples but also an interagglomerates sintering. The modification of the porosity allows an easier release of the formed gaseous compounds and a regular and more significant shrinkage leading to higher sintered densities (87% TD). Compared with non-ground samples, the remaining whole porous volume is half as low, but it corresponds principally to a higher closed porous volume, due to the presence of small closed pores.

Therefore, the ball-milling of the precursors appears as an essential step of the procedure of preparation of high-density ceramic bodies by sintering 3 mol% Y_2O_3–ZrO_2 powders synthesized by the acetate route.

As for the pH of formation of the precursors, it has limited influence on the sintered densities, although at equal whole porous volume, the pH increase seems to favour the formation of closed pores, which could be considered as a disadvantage. In other respects, however, the pH increase makes the filtration and washing of precursors easier. Consequently, formation of gels at basic pH has to be preferred and after optimization of the procedure including a careful washing of the precursors, sintered densities reaching 94·8% of the theoretical density have been achieved (Samdi, A., unpublished).

References

1. Samdi. A., Grollier-Baron, T., Durand, B. & Roubin, M., Préparation, par hydrolyse de solutions aqueuses, d'acétate de zirconium et d'yttrium précurseurs de zircones dopées à l'yttrium finement divisées. *Ann.Chim. Fr.*, **13** (1988) 517-26.
2. Samdi, A., Durand, B., Roubin, M., Daoudi, A., Taha, M., Paletto, J. Fantozzi. G., Pressing and sintering behaviour of yttria stabilized zirconia powders prepared from acetate solutions. *J. Eur. Ceram. Soc.* **12** (1993) 353–60.
3. Samdi, A., Grollier-Baron, T., Durand, B. & Roubin M.,

Elaboration de poudres finement divisées de zircone pure à partir d'acétate de zirconium cristallisé. *Ann. Chim. Fr.*, **13** (1988) 171–87.
4. Samdi, A., Grollier-Baron, T., Durand, B. & Roubin, M., Elaboration de poudres finement divisées de zircone pure à partir d'acétate de zirconium amorphe. *Ann. Chim. Fr.*, **13** (1988) 471–82.
5. Van De Graaf, M. A. C. G., Ter Maat, J. H. H. & Burgraaf, A. J., Microstructural development during pressing and sintering of ultrafine zirconia powders. In *Ceramic Powders*. Elsevier, Amsterdam, 1983, pp. 783–94.
6. Dimilia, R. A. & Reed, J. S., Dependence of compaction on the glass transition temperature on the binder phase. *Ceram. Bull.*, **62**(4) (1983) 484–8.
7. Descemond, M., Durand, B., Samdi, A., Brodhag, C., Thevenot, F. & Roubin, M., Influence of elaboration conditions on the densification of zirconia powders obtained from acetates. *J. Mat. Sci.*, **28** (1993) 3754–60.